

Modeling of Packed Bed Reactors: Hydrogen Production by the Steam Reforming of Methane and Glycerol

A. G. Dixon^{*1}, B. MacDonald¹, A. Olm¹

¹Department of Chemical Engineering, Worcester Polytechnic Institute, Worcester, MA, USA

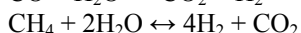
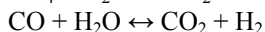
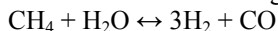
*Corresponding author: agdixon@wpi.edu

Abstract: COMSOL Multiphysics was used to model methane steam reforming (MSR) and glycerol steam reforming (GSR) in a fixed bed reactor of tube-to-particle diameter ratio $N = 5.96$. The calculations were made using a steady-state 1D heterogeneous model, made up of an effective medium reactor tube model coupled to a single spherical pellet model for the source term at each point of the tube. The focus of the present paper is to show how to include the effects of mole changes due to reaction on the reforming processes in the absence of heat effects. The changes in gas density and velocity are accounted for by tracking changes in pressure and mean molar mass along the tube. The implementation of this multi-geometry model in COMSOL Multiphysics is discussed, and two different approaches to accounting for the mole changes are compared.

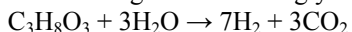
Keywords: Reaction engineering, packed bed, hydrogen production, methane steam reforming, glycerol steam reforming

1. Introduction

The production of hydrogen is important in the chemical industry; applications include hydrotreating and energy conversion by fuel cells. The conventional route is by the endothermic steam reforming of methane (MSR)



in a multitubular packed bed, at > 20 bar and $700\text{-}800$ °C and using high flow rates. With the increasing use of biodiesel as a renewable fuel, interest has grown in producing hydrogen by steam reforming of the excess glycerol (GSR)



which is produced as a side product. This endothermic reaction also takes place at high temperature but at lower pressures (see Table 1 in the Appendix for values).

Packed beds are important in the chemical industries in separations and as catalytic reactors.

The standard approach to modeling the complex particle/tube arrangement in a packed bed is to employ an effective medium approach with one-dimensional flow and lumped transport parameters. Simplification of the flow and estimation of the transport quantities is usually done by experiment and empiricism.

The aim of our research is to use COMSOL Multiphysics to model a tubular packed bed reactor where the tube is an effective medium, with the reaction rates obtained by solving a single pellet model at each point [1]. The reforming reactions studied involve changes in moles, and a rigorous treatment of the effects of this on velocity and conversion is presented. In this paper we calculate the impact of the mole changes in the absence of heat effects, so the simulations reported here are isothermal. We illustrate the approach using a one-dimensional domain for the reactor tube coupled to a 2D domain for the single particle model [2] in COMSOL

2. Model Equations

The model equations are given here in dimensional form. Axial dispersion is included, as is axial variation of pressure along the tube. The catalyst pellet was taken to have spherical symmetry.

2.1 Ergun equation for pressure drop

The pressure drop in the packed column is described by the differential form of the Ergun equation:

$$-\frac{dP}{dz} = \frac{(1 - \varepsilon_b)G}{d_p \varepsilon_b^3 \rho} \left[150 \frac{(1 - \varepsilon_b)\mu_f}{d_p} + 1.75G \right] \quad (1)$$

where P is pressure (Pa), z is the reactor axial coordinate (m), ε_b is the average bed voidage, G is the mass flux ($\text{kg/m}^2\text{s}$), d_p is the catalyst pellet

diameter (m), μ_f is the fluid viscosity (kg/m·s), and ρ is the fluid density (kg/m³).

2.2 Catalyst pellet species balances

Concentration profiles were computed for five components in the MSR case and four components for GSR. The profiles were based on the following material balances accounting for reaction, convection and Fickian diffusion in the spherical catalyst domain:

$$\frac{1}{r^{*2}} \frac{d}{dr^*} \left(D_{pi} r^{*2} \frac{dc_{pi}}{dr^*} \right) = - \sum_{j=1}^{NR} \alpha_{ij} r_j \quad (2)$$

where r^* represents the radial position within the pellet (m), D_{pi} represents the diffusivity of component i in the pellet (m²/s), C_{pi} represents the concentration of component i in the pellet (mol/m³), α_{ij} represents the stoichiometric coefficient of component i in reaction j , and r_j represents the rate of reaction j (mol/m³s).

2.3 Gas phase species balances

The concentration profiles in the reactor bulk gas phase are described by

$$\frac{1}{A_c} \frac{dF_i}{dz} - a_p (1 - \varepsilon_b) k_g (C_{pi}^s - c_i) = D_{ea} \frac{d^2 c_i}{dz^2} \quad (3)$$

where A_c is the cross-sectional area of the reactor tube (m²), F_i is the molar flow rate of component i (mol/s), a_p is the ratio of the pellet's surface area to volume (m⁻¹), k_g is the particle-to-fluid mass transfer coefficient (m/s), C_{pi}^s is the concentration of component i at the pellet surface (mol/m³), c_i is the concentration of component i in the gas (mol/m³), and D_{ea} is the reactor axial dispersion coefficient (m²/s).

Equation (3) is not in the form required by COMSOL, as there are two dependent variables F_i and c_i which are related by

$$F_i = c_i u A_c \quad (4)$$

Two approaches can be used to address this problem. In the first approach [3], we can write, assuming constant A_c

$$\frac{1}{A_c} \frac{dF_i}{dz} = \frac{d(c_i u)}{dz} = u \frac{dc_i}{dz} + c_i \frac{du}{dz} \approx u \frac{dc_i}{dz} \quad (5)$$

After substituting for the first term in equation (3), c_i is the only dependent variable; the equation is solved for $i = 1, \dots, N_s$. Then the equations

$$c_{tot} = \sum_{i=1}^{N_s} c_i, \quad u = u_f \frac{c_{tot} P_f}{c_f P} \quad (6)$$

are used to account for the change in velocity u due to mole changes and pressure drop.

The above approximation provides a convenient way to deal with mole changes; however, the drawback is that the total concentration is not constrained to satisfy the ideal gas law (or other equation of state). A different approach [4] follows from writing

$$\begin{aligned} \frac{1}{A_c} \frac{dF_i}{dz} &= \frac{d(c_i u)}{dz} = \frac{d(y_i c_{tot} u)}{dz} \\ &= \frac{d}{dz} \left(y_i \frac{\rho}{M} u \right) = G \frac{d}{dz} \left(\frac{y_i}{M} \right) \end{aligned} \quad (7)$$

where

$$M = \sum_{i=1}^{N_s} y_i M_i, \quad \frac{dM}{dz} = \sum_{i=1}^{N_s} M_i \frac{dy_i}{dz} \quad (8)$$

are the mean molar mass and its derivative, and G is the constant mass flux (kg/m²·s). If we write Fick's law correctly as

$$J_i = -c_{tot} \nabla \cdot (D_{ea} \nabla y_i) \quad (9)$$

then for the gas phase species balance we get

$$\begin{aligned} -c_{tot} D_{ea} \frac{d^2 y_i}{dz^2} - \frac{y_i G}{M^2} \frac{dM}{dz} + \frac{G}{M} \frac{dy_i}{dz} \\ = a_p (1 - \varepsilon_b) k_g (C_{pi}^s - c_{tot} y_i) \end{aligned} \quad (10)$$

for $i = 1, 2, \dots, N_s - 1$. This is supplemented by

$$\sum_{i=1}^{N_s} y_i = 1, \quad c_{tot} = \frac{P}{RT}, \quad u = \frac{G}{c_{tot} M} \quad (11)$$

2.4 Boundary conditions

At the tube inlet we take

$$P = P_f, \quad y_i = y_{if} \quad (12)$$

while at the tube exit the outflow condition

$$-D_{ea} \frac{dy_i}{dz} = 0 \quad (13)$$

was imposed. For the pellet equations there was symmetry at $r^* = 0$, while at the pellet-gas interface equating the fluxes gave

$$-D_{pi} \frac{dC_{pi}}{dr^*} \Big|_{r^*=R_p} = k_g (C_{pi}^s - c_{tot} y_i) \quad (14)$$

3. Use of COMSOL Multiphysics

Our approach follows that of the Packed Bed Reactor example in the COMSOL User Guide [3], but with a modified treatment of mole changes. Two model domains were used, a line for the 1-D tube and a square for the 2-D spherical particle model, connected by coupling variables (Figure 1). The coordinates r^* and z were scaled by $x = z/L$ and $y = r^*/R_p$. In the gas phase the concentration variable was defined by

$$c_i^*(x) = y_i(x) \frac{P_f}{RT} \quad (15)$$

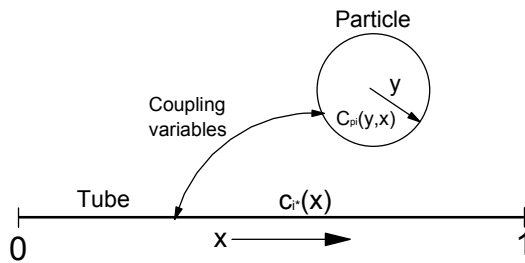


Figure 1. Schematic of tube-particle models

Tube pressure drop was calculated by the Ergun equation using the Coefficient PDE feature of COMSOL. The equations for diffusion and reaction in the pellet and convective dispersion in the tube were handled by use of COMSOL Multiphysics and the Chemical Reaction Engineering Module.

Literature kinetics were available for both the MSR [5] and GSR [6, 7] reactions. The kinetic constants are available in the original references. Standard correlations were used for the axial dispersion coefficient D_{ea} [8]:

$$\frac{ud_p}{D_{ea}} = \frac{0.73\epsilon}{ReSc} + \frac{0.5}{1 + \frac{9.7\epsilon}{ReSc}} \quad (16)$$

and the particle-gas mass transfer coefficient k_g [9]:

$$\frac{k_g d_p}{D_{AB}} = 2 + 1.1 Re^{0.6} Sc^{0.33} \quad (17)$$

The tube model equation requires the species fluxes from the pellet surface as a source term, and these were made available using coupling variables [3]. Likewise the pellet equations require the tube bulk concentrations as boundary conditions, and again coupling variables were used. Figure 2 shows schematically how this was set up in COMSOL Multiphysics.

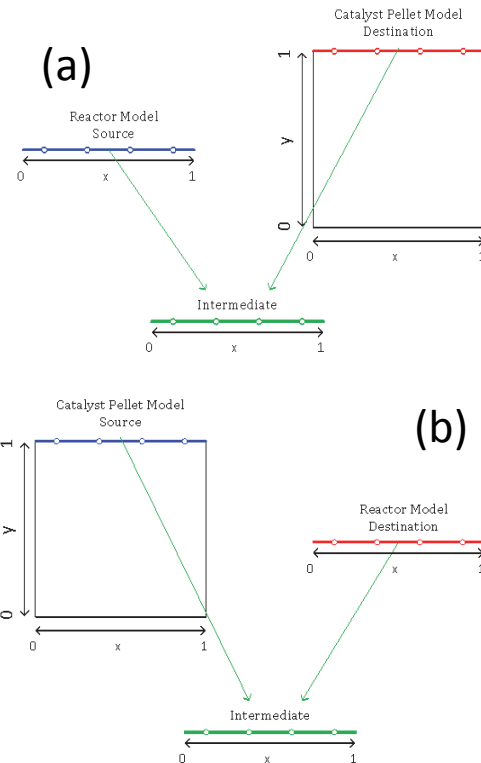


Figure 2. Coupling scheme to supply tube concentrations to particle fluxes (a) and to supply particle surface fluxes to tube balance (b)

The domains were meshed using 100 uniform elements for the 1D tube model, while in the 2D pellet model the same 100 elements were used in the x -direction, and 60 elements were used in the y -direction. The y -direction mesh was distributed so that it was refined near the pellet surface, using a geometric sequence with an element ratio of 0.1. A typical MRS solution used 34,010 degrees of freedom and GSR used 25,249.

4. Results and Discussion

The results first show the consequences of using the concentration-based approach, then results for MSR and GSR are presented using the molar mass method advocated here.

4.1 Approach using equations (5) and (6)

A major drawback of the approach using c_i as dependent variables as in equations (5) and (6) is that the total concentration is not forced to satisfy the equation of state. This is illustrated for MSR in Figure 3.

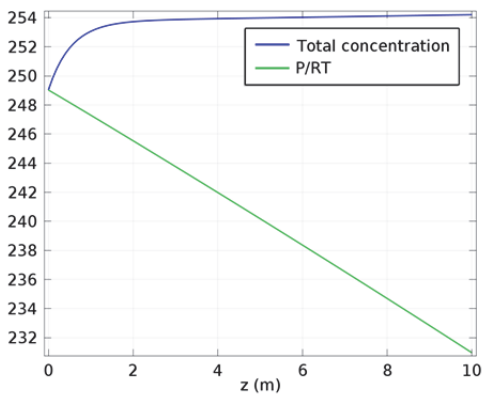


Figure 3. Comparison of c_{tot} for MSR using the two methods described in this paper

The figure shows that the expression P/RT decreases along the reactor tube due to the pressure drop in this isothermal simulation. The quantity c_{tot} which is calculated as in equation (6) is seen to continually increase, which is not the expected behavior on physical grounds.

4.2 MSR simulation

Figure 4 shows the concentration of methane in the two-dimensional pellet domain. Along the x -coordinate at $y = 1$ we see that the surface concentration of CH_4 decreases monotonically down the reactor tube as the reactant is used up. Along the y -coordinate at low values of x we see a sharp drop near the pellet surface, due to the strong diffusion limitations for this reaction. Inside the pellet the reaction reaches equilibrium and the CH_4 concentration is constant.

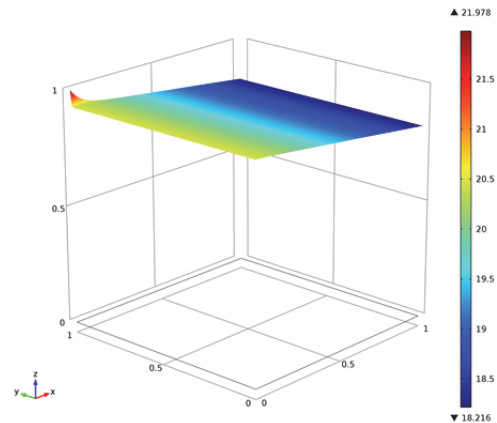


Figure 4. CH_4 concentration inside the catalyst pellet (y -coordinate is r^*/R_p) and along the tube (x -coordinate is z/L) for MSR

To illustrate the effect of pressure, the MSR simulation was run twice, once with the pressure drop computed by the Ergun equation, and once with pressure constant at the inlet value. A comparison for CH_4 conversion is shown in Figure 5.

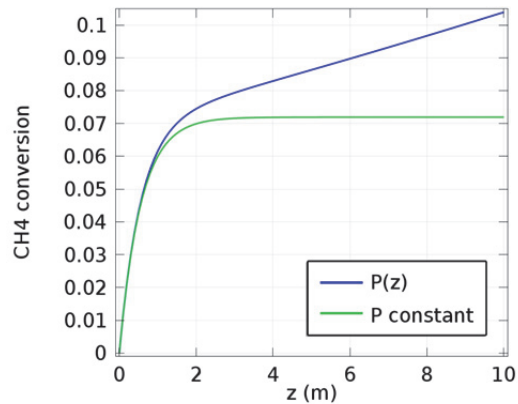


Figure 5. Axial profile of CH_4 conversion for MSR comparing actual to zero pressure drop cases

For both cases, the CH_4 conversion increases at first due to the initial consumption of reactant in the tube. For constant pressure, it then levels out as the reactions come to equilibrium. For the case with pressure drop, equilibrium conversion slowly increases following Le Chatelier's principle due to the lower pressure.

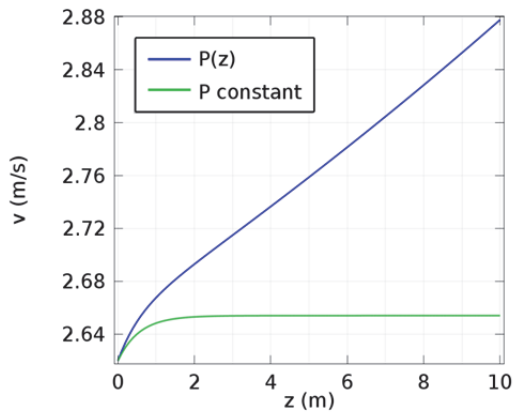


Figure 6. Velocity profile along tube for MSR, comparing actual to zero pressure drop cases

Figure 6 shows how the linear velocity changes for the same two cases with and without pressure drop. The conversion in the MSR case is relatively low, so in the absence of pressure effects the velocity change due to the increase in moles is small, only about 1%. Similarly the change in mean molar mass is small. The larger change seen for the pressure drop case is about 8-9%, mostly caused by the change in pressure through c_{tot} in equation (11).

4.3 GSR simulation

Figure 7 shows the concentration of glycerol in the two-dimensional pellet domain.

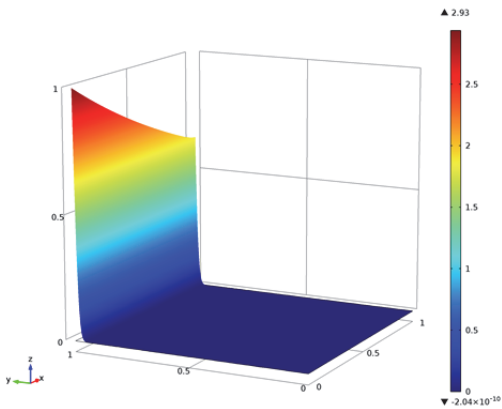


Figure 7. $C_3H_8O_3$ concentration inside the catalyst pellet (y -coordinate) and along the tube (x -coordinate) for GSR.

Along the x -coordinate at $y = 1$ we see that the surface concentration of $C_3H_8O_3$ decreases

more strongly down the reactor tube as the GSR reaction rate is higher than that of MSR. Along the y -coordinate we see a very sharp drop near the pellet surface, due to the even stronger diffusion limitations in GSR than in MSR. Inside the pellet the $C_3H_8O_3$ concentration drops to zero as the reaction is modeled as being irreversible and thus complete conversion is possible.

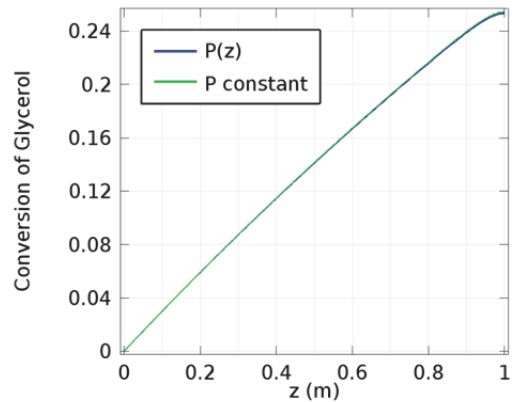


Figure 8. Axial profile of $C_3H_8O_3$ conversion for GSR comparing actual to zero pressure drop cases

For the GSR reaction the pressure drop is lower than for MSR. Both glycerol conversion and mean molar mass are virtually unaffected by the pressure drop along the tube (Figures 8 and 9). The glycerol conversion reaches 25% in only a 1 m long reactor. The mean molar mass decreases by 12% in this case.

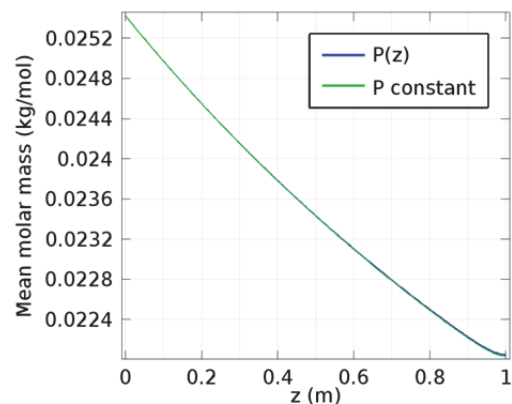


Figure 9. Axial profile of mean molar mass for GSR comparing actual to zero pressure drop cases

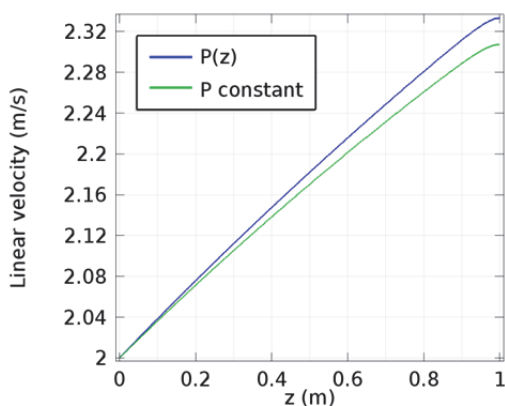


Figure 10. Axial profile of linear velocity for GSR comparing actual to zero pressure drop cases

Changes in linear velocity in these isothermal simulations are due to both changes in pressure and to changes in moles due to the stoichiometry of the reactions. For MSR the changes seen in linear velocity were relatively small and were due almost entirely to the pressure drop. The changes in linear velocity shown in Figure 10 for the GSR reaction, on the other hand, were mainly due to the change in moles in the GSR reaction. This also explains the similar behavior in the pressure drop and constant-P cases.

5. Conclusions

The effects of mole increases on the gas velocity and conversion for MSR and GSR were simulated rigorously using the variable mean molar mass. Results are reported for isothermal 1-D calculations; future papers will present results for 2-D non-isothermal cases.

6. References

- Allain, F.; Dixon, A. G., Modeling of transport and reaction in a catalytic bed using a catalyst particle model, Proceedings of the COMSOL Conference, Boston (2010)
- Petera, J.; Nowicki, L.; Ledakowicz, S., New numerical algorithm for solving multidimensional heterogeneous model of the fixed bed reactor, *Chem. Eng. J.* **214**, 237-246 (2013)
- COMSOL Multiphysics Model Library, Chemical Reaction Engineering Module, Packed bed reactor, Version 4.3b, COMSOL AB (2013)

- Cropley, J. B.; Burgess, L. M.; Loke, R. A., The optimal design of a reactor for the hydrogenation of butyraldehyde to butanol, *ACS Symp. Ser.*, **237**, 255-270 (1984)
- Hou, K.; Hughes, R., The kinetics of methane steam reforming over a Ni/ α -Al₂O₃ catalyst, *Chem. Eng. J.*, **82**, 311-328 (2001)
- Cheng, C. K.; Foo, S. Y.; Adesina, A. A., Glycerol steam reforming over bimetallic Co-Ni/Al₂O₃, *Ind. Eng. Chem. Res.*, **49**, 10804-10817 (2010)
- Iliuta, I.; Iliuta, M.; Radfarnia, H., Hydrogen production by sorption-enhanced steam glycerol reforming: sorption kinetics and reactor simulation, *AIChE J.*, **59**, 2105-2118 (2013)
- Edwards, M. F.; Richardson, J. F., Gas dispersion in packed beds, *Chem. Eng. Sci.*, **23**, 109-123 (1968)
- Wakao, N.; Funazkri, T., Effect of fluid dispersion coefficients on particle-to-fluid mass transfer coefficients in packed beds, *Chem. Eng. Sci.*, **33**, 1375-1384 (1978)

7. Acknowledgements

Some of the preliminary calculations for glycerol steam reforming were made by John E. Kent in his senior year qualifying project.

8. Appendix

Table 1: Constants used in MSR and GSR models

Quantity (f : feed)	MSR	GSR
L	10 m	1 m
d_p	0.0254 m	0.0200 m
R	0.075692 m	0.0596 m
u_f	2.62 m/s	2.00 m/s
k_g	0.1378 m/s	0.618 m/s
D_{ea}	0.033 m ² /s	0.0663 m ² /s
ρ_f	3.87 kg/m ³	0.75 kg/m ³
μ	3.78×10^{-5} kg/m·s	2.74×10^{-5} kg/m·s
T	1019.05 K	823 K
P_f	21.1 bar	2.02 bar